IEEE Access
Multidisciplinary | Rapid Review | Open Access Journal

Date of publication xxxx 00, 0000, date of current version xxxx 00, 0000.

Digital Object Identifier 10.1109/ACCESS.2017.DOI

Channel Capacity Analysis of A Comprehensive Absorbing Receiver for Molecular Communication via Diffusion

SHENGHAN LIU[1], ZHUANGKUN WEI[2], XIANG WANG[3] AND CHENGLIN ZHAO[1].
[1]School of Information and Communication Engineering, Beijing University of Posts and Telecommunications, Beijing, 100876, China.
[2]School of Engineering, University of Warwick, Coventry CV4 7AL, U.K.
[3]Beijing Jianyi Corporation, Ltd., Beijing, 100089, China.

Corresponding author: Shenghan Liu (night_several@bupt.edu.cn)

This work was supported in part by the National Natural Science Foundation of China (NSFC) under Grant 61971050, U1805262 and in part by 2019 Industrial Internet Innovation Development Project of Ministry of Industry and Information Technology of P.R. China "Comprehensive Security Defense Platform Project for Industrial/Enterprise Networks".

ABSTRACT As a promising communication paradigm, Molecular Communication (MC) has been developing for more than ten years. During this period, with the continually development and mature of molecular channel, more and more factors from the actual molecular environment are taken into account to model the molecular channel more precisely. Due to the fact that chemical reactions are common and crucial in molecular communication environment, this paper investigates the impacts of various reaction rates on the channel modeling and channel capacity of MC. First, a detailed molecular system model is presented with a first-order degradation reaction in the channel and a second-order reversible reaction at the receiver side. Because of the Inter-Symbol Interference (ISI) induced by the stochastic nature of molecule motions, we propose an approximation method with low complexity to describe the received molecule signal with an arbitrary length of ISI. Based on the noisy molecular signal, closed-form expressions for probabilities of detection and false alarm are derived. The performance of channel capacity is evaluated concentrating on different circumstances with decoupled reaction rates and two prevalent modulation techniques (BCSK and MoSK) are implemented to ensure the accuracy and scientific of the conclusion. Numerical results show that the channel capacity could be enhanced significantly by selecting proper messenger molecules with desirable reaction rates in specific molecular channel.

INDEX TERMS Molecular Communications, degradation reaction, reversible reaction, modulation technique, reaction rates, channel capacity.

I. INTRODUCTION

MOLECULAR communication systems are widespread among cells and organisms at nano-scale in biology, attracting a large number of researchers to be engaged in interdisciplinary research and cooperation recently [1]–[3]. Meanwhile, MC is widely applied to the field of environmental monitoring, biological detection and disease treatment, due to the environment in which it exists and biocompatibility [4]–[6].

Unlike traditional wireless communication, MC adopts molecules as carriers to deliver information [7]. Furthermore, the transmitter and the receiver in a typical MC system are suspended in an aqueous or a gaseous environment [8]. A variety of molecular channels has been found and modeled [9]–[19], which is divided into two major categories: passive diffusion and active transport. The former one refereed to as Molecular Communication via Diffusion (MCvD) attracts more researchers' attention because the diffusion-based molecular channel does not require any additional facilities, saving the cost of both equipment and energy.

For the sake of reasonably designing modulation, coding and detection mechanism of MCvD, accurate molecular channel model as well as Channel Impulse Response (CIR) are essential in most scenarios [20], [21]. After years of research, the molecular channel model has become more and more complicated considering more physiological and chemical mechanisms in the actual cell environment.

Initially, the researchers focus on the passive molecular

This article has been accepted for publication in a future issue of this journal, but has not been fully edited. Content may change prior to final publication. Citation information: DOI 10.1109/ACCESS.2020.3045439, IEEE Access

receiver, assuming that the receiver is transparent and the signal is represented by quantity (e.g. concentration) or structure (e.g. type) characteristics of messenger molecules inside the receiver [9]. Nevertheless, the passive model is lack of interpreting ability to account for how the receiver senses and receives the messenger molecules. With the in-depth research, a fully-absorbing receiver model is proposed in [10]. In this situation, messenger molecules released by the transmitter are absorbed by the receiver through binding reactions once they hit the surface of receiver, and a closed-form analytical expression for the number of absorbed molecules varying over time is derived. However, a collision between a messenger molecule and the receiver surface does not necessarily form an absorption process, the reaction follows the principle of ligand-receptor binding kinetics [11], [12], where the receptors are distributed on the surface of receiver. The messenger molecule could react with the receptor via a second-order reversible reaction [13]. Some researches are inspired by this mechanism such as the consideration of the number and size of receptors [14]. Moreover, during the propagation, messenger molecules may be degraded through certain reaction in the bio-environment such as enzyme mechanism [15], [16], which enlightens the authors in [17] and [18] to study the effect of a limited amount and the deployment of enzymes respectively. Based on above considerations, a comprehensive molecular absorbing receiver model is researched by the authors in [19], taking into account the reaction process of the messenger molecules both during the propagation and on the surface of receiver. Unfortunately, this work focuses most on the channel model but does not study the channel capacity with continuous molecular signals.

In fact, the reactions occurred in the channel have a great influence on CIR, which would further affect the continuous molecular signals. Thus it is quite necessary to evaluate the impacts of various reaction rates on the quality of communication, assisting to select proper messenger molecules for communication in specific environment.

Our main contributions in this paper are listed as follows:

(1) We first investigate the channel model with a first-order degradation reaction and a second-order reversible reaction in detail, then the analytical expressions for the CIR under variable circumstances of reaction rates are derived.

(2) Given the CIR of each case, we derive the total number of messenger molecules received by the receiver considering all the ISI and the background noise in a low complexity manner employing normal approximation. On this foundation, the probabilities of detection and false alarm are derived for two modulation techniques (BCSK and MoSK) to ensure the validity and universality.

(3) Numerical results obtained by particle-based simulations are provided, which indicates that different reaction rates have various impacts on the CIR and the performance of channel capacity. Moreover, the effective length of ISI is influenced by the reaction rates as well.

The remainder of this paper is organized as follows. The system model is described in Section II. In Section III, the molecular signal modeling, modulation techniques and the conditional probabilities are elaborated in detail. The numerical results are shown in Section IV. Lastly, we conclude our paper in Section V.

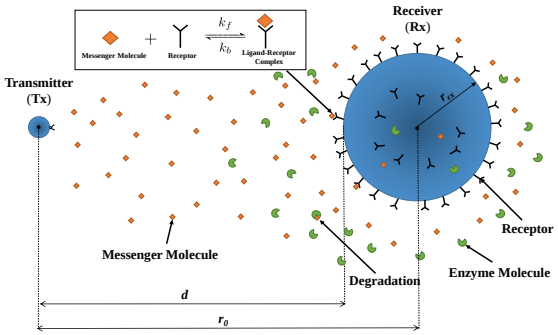

FIGURE 1. A typical MCvD channel model in 3-D fluid environment.

II. CHANNEL MODEL AND ANALYTICAL EXPRESSIONS

A. CHANNEL MODEL

In this subsection, an end-to-end MCvD channel is considered which includes a point transmitter (Tx) and a spherical receiver (Rx) of radius r_{rx}, as sketched in Fig. 1. The transmitter and the receiver are fixed and stable (i.e., can not be moved or destroyed) during the communication. The channel is present in an unbounded 3-D environment full of a homogeneous fluid medium with constant viscosity and temperature, which means the overall temperature of the environment wouldn't be changed by chemical reactions occurred during the communication. The transmitter is located at distance r_0 from the center of the receiver and we define the distance from the transmitter to the closest point on the surface of the receiver as d, where $d = r_0 - r_{rx}$. The molecules released from Tx diffuse into the environment through Brownian motion [22] with diffusion coefficient D until absorbed by Rx. The diffusion coefficient is a physical quantity indicating the degree of molecular diffusion. The motion of each messenger molecule is independent of each other, and the collision between them could be ignored since the size of them is negligible [23]. The diffusion coefficient is determined by the temperature T and viscosity η of the medium, the radius of messenger molecule r_{mm} and Boltzmann constant k_B:

$$D = \frac{k_B T}{6\pi\eta r_{mm}} \tag{1}$$

Without loss of generality, we regard A molecules as the messenger molecules to study the propagation and absorbing properties. During the propagation, A molecules may be degraded via certain chemical reactions such as the enzyme reaction:

$$E + A \underset{k_{-1}}{\overset{k_1}{\rightleftharpoons}} EA \overset{k_p}{\rightleftharpoons} E + A_P \tag{2}$$

This article has been accepted for publication in a future issue of this journal, but has not been fully edited. Content may change prior to final publication. Citation information: DOI 10.1109/ACCESS.2020.3045439, IEEE Access

where E, EA, A_P, and k_{-1}, k_1, k_p are the enzyme, enzyme-messenger molecule complex, product, and reaction rates respectively. The assumptions in [15] are adopted which assume that the degradation rate is relatively very fast and the reversible rate is relatively very slow, i.e. $k_p \to \infty$ and $k_{-1} \to 0$. Thus the reaction equation is simplified as:

$$A \xrightarrow{k_d} A_P \tag{3}$$

where k_d is the first-order degradation reaction rate in s^{-1} and A_P is the product of the reaction which is unable to be absorbed or recognized by Rx.

Each messenger molecule that successfully arrives at the receiver may react with the receptor covered on the surface of the receiver, forming a ligand-receptor complex molecule to retrieve the original information, via a second-order reversible reaction in the form as:

$$A + R \underset{k_b}{\overset{k_f}{\rightleftharpoons}} C \tag{4}$$

where k_f is the forward reaction rate in $m^3 s^{-1}$ and k_b is the backward reaction rate in s^{-1}. R and C denote the receptor and the ligand-receptor complex respectively. In order to obtain the analytical expression of CIR and analyze the effect of reaction rate on the performance of information transmission, the receiver is regarded as a fully absorbing model. Under this condition, the messenger molecules could react with the receptor once they reach the surface of the receiver. Besides, once a messenger molecule is separated from the receptor, it continues moving in the manner of Brownian Motion until degraded or recombining with a receptor again.

B. ANALYTICAL EXPRESSIONS

The CIR of the considered MCvD system is defined as the probability of a messenger molecule released from Tx forming a molecule C during the time interval t (start with $t = 0$), denoted by $P(r, t)$. In three-dimensional channel environment, the Brownian motion of messenger molecules obeys the Fick's Second Law and is restricted by degradation reaction in (3):

$$\frac{\partial(r \cdot P(r,t))}{\partial t} = D \cdot \frac{\partial^2(r \cdot P(r,t))}{\partial r^2} - k_d \cdot P(r,t) \tag{5}$$

Equation (5) satisfies the following initial conditions:

$$\begin{aligned} &P(r, t \to 0) = \frac{1}{4\pi r_0^2}\delta(r - r_0) \\ &P(r \to \infty, t|r_0) = 0 \end{aligned} \tag{6}$$

where $\delta(\cdot)$ is the Dirac function, and the two initial conditions correspond to the states of messenger molecules at Tx and at the infinite distance, respectively. At the receiver, the reversible reaction between the messenger molecule and receptor is expressed by the following equation:

$$\begin{aligned} D\frac{\partial(P(r_{rx},t))}{\partial r} &= k_f P(r_{rx}, t) \\ &- k_b \int_0^t D\frac{\partial(P(r_{rx},\tau))}{\partial r} d\tau \end{aligned} \tag{7}$$

where r_{rx} denotes the radius of Rx. Since the number of molecule C on the surface of Rx is zero at $t = 0$, the following initial conditions exist:

$$P(r_{rx}, 0) = 0 \tag{8}$$

Given the assumptions above, the CIR of the considered MCvD system is derived as [19]:

$$\begin{aligned} P(r,t) =& \frac{k_f \exp(-k_d t)}{4\pi r_0 r_{rx}\sqrt{D}} \left\{ \frac{\alpha \mathrm{W}\left(\frac{d}{\sqrt{4Dt}}, \alpha\sqrt{t}\right)}{(\gamma-\alpha)(\alpha-\beta)} \right. \\ &\left. + \frac{\beta \mathrm{W}\left(\frac{d}{\sqrt{4Dt}}, \beta\sqrt{t}\right)}{(\beta-\gamma)(\alpha-\beta)} + \frac{\gamma \mathrm{W}\left(\frac{d}{\sqrt{4Dt}}, \gamma\sqrt{t}\right)}{(\beta-\gamma)(\gamma-\alpha)} \right\}, \end{aligned} \tag{9}$$

where we define $\mathrm{W}(a,b) = \exp(2ab + b^2) \cdot \mathrm{erfc}(a + b)$, and $\mathrm{erfc}(\cdot)$ is referred to as the complementary error function. The constants α, β, and γ are the solutions of the following equations:

$$\begin{cases} \alpha + \beta + \gamma = \left(1 + \dfrac{k_f}{4\pi r_{rx} D}\right)\dfrac{\sqrt{D}}{r_{rx}}, \\ \alpha\gamma + \beta\gamma + \alpha\beta = k_b - k_d, \\ \alpha\beta\gamma = k_b \dfrac{\sqrt{D}}{r_{rx}} - k_d\left(1 + \dfrac{k_f}{4\pi r_{rx} D}\right)\dfrac{\sqrt{D}}{r_{rx}}. \end{cases} \tag{10}$$

In the remainder of this subsection, we investigate the CIR of the MCvD system in three circumstances, in which we focus on the impact of specific reaction rate.

1) First-Order Degradation Reaction Rate

In the molecular channel, the degradation rate k_d depends on the concentration and distribution of enzymes in the channel [24]. In order to investigate the effect of degradation rate on CIR, the reversible reaction in (4) is simplified as a one-way reaction, and it is assumed that the forward and backward reaction rates are infinite and zero respectively, i.e., $k_f \to \infty$ and $k_b = 0$. It is readily to see that the solutions to the equations in (10) are:

$$\alpha \to \infty, \beta = \sqrt{k_d}, \gamma = -\sqrt{k_d}. \tag{11}$$

After substituting the solutions into (9), the CIR simplifies to:

$$\begin{aligned} P(r,t) =& \frac{r_{rx}}{2r_0}\left\{ \exp\left(-d\sqrt{\frac{k_d}{D}}\right) \times \mathrm{erfc}\left(\frac{d}{\sqrt{4Dt}} - \sqrt{k_d t}\right) \right. \\ &\left. + \exp\left(d\sqrt{\frac{k_d}{D}}\right) \times \mathrm{erfc}\left(\frac{d}{\sqrt{4Dt}} + \sqrt{k_d t}\right) \right\}. \end{aligned} \tag{12}$$

2) Second-Order Forward Reaction Rate

At the receiver, the forward reaction rate k_f is mainly related to the size of the receptor and the activation energy in the process of ligand receptor binding [25]. In order to study the influence of forward reaction rate on CIR, it is necessary to eliminate the interference of degradation reaction rate and backward reaction rate. In this situation, we also consider

This article has been accepted for publication in a future issue of this journal, but has not been fully edited. Content may change prior to final publication. Citation information: DOI 10.1109/ACCESS.2020.3045439, IEEE Access

the one-way reaction, and we assume that the messenger molecules won't be degraded during the propagation, i.e., $k_d = 0$, $k_f > 0$ and $k_b = 0$. It is shown that the solutions to the equations in (10) are:

$$\alpha = \left(1 + \frac{k_f}{4\pi r_{rx} D}\right) \frac{\sqrt{D}}{r_{rx}}, \beta = 0, \gamma = 0. \tag{13}$$

The CIR is simplified by substituting the values of α, β and γ into (9), as:

$$P(r,t) = \frac{k_f r_{rx}}{r_0(k_f + 4\pi r_{rx} D)} \left\{ -\mathrm{W}\left(\frac{d}{\sqrt{4Dt}}, \alpha\sqrt{t}\right) + \mathrm{erfc}\left(\frac{d}{\sqrt{4Dt}}\right) \right\}. \tag{14}$$

3) Second-Order Backward Reaction Rate

In molecular channel, the backward reaction rate k_b mainly depends on the stability of chemical bond between the ligand and receptor [26]. In the research on the backward reaction rate, it is first assumed that $k_d = 0$, $k_f > 0$ and $k_b > 0$ to obtain a feasible solution for (10). Although no obvious solution could be obtained from (10) directly, fortunately, due to the special symmetric cycle characteristics of the equation, a set of trivariate cubic equations could be solved to get the value of α, β and γ. Equation (10) is thus simplified as a unary cubic equation:

$$x^3 - \left(1 + \frac{k_f}{4\pi r_{rx} D}\right) \frac{\sqrt{D}}{r_{rx}} x^2 + k_b x - k_b \frac{\sqrt{D}}{r_{rx}} = 0. \tag{15}$$

Suppose that x_1, x_2, x_3 are the three solutions of a unary cubic equation:

$$x^3 + bx^2 + cx + d = 0, \tag{16}$$

then we have $(x-x_1)(x-x_2)(x-x_3) = 0$ with its expansion as:

$$x^3 + (-x_1 - x_2 - x_3)x^2 + (x_1x_2 + x_1x_3 + x_2x_3)x - x_1x_2x_3 = 0, \tag{17}$$

by comparing (17) with (16), the coefficients of (16) are:

$$\begin{cases} x_1 + x_2 + x_3 = -b, \\ x_1x_2 + x_1x_3 + x_2x_3 = c, \\ x_1x_2x_3 = -d. \end{cases} \tag{18}$$

Solving (10) is much more simpler via Cardano's method or Vieta's method [27], and the roots here are α, β and γ respectively.

It is worth noting that in the vast majority of the literatures for MC, the CIR is defined as the variation of the number of received messenger molecules (i.e., the number of molecule C) over time t. To be consistent with them, we use $\frac{\partial P(r,t)}{\partial(t)}$ as the CIR in Section IV.

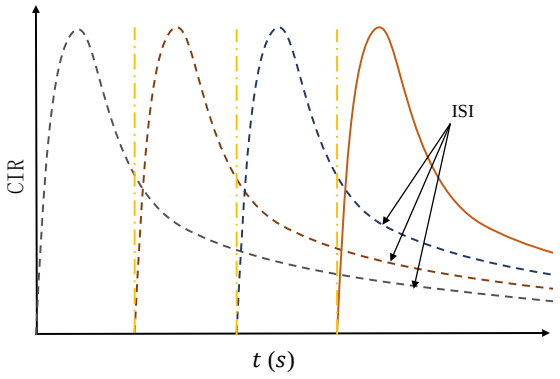

FIGURE 2. A schematic diagram of ISI in molecular channel.

III. PRELIMINARIES AND MODULATION TECHNIQUES

A. PRELIMINARIES

During the communication, it is assumed that the time is divided into equal sized slots, i.e., symbol interval T_s. At the beginning of each time slot, N_0 messenger molecules are released by the transmitter to represent bit '1' with a priori probability π_1, whereas no molecule is released to represent bit '0' with probability π_0. When N_0 molecules are released, since each molecule moves independently, the number of received molecules by the receiver follows the binomial distribution as $\mathcal{B}(N_0, P(r,t))$, where $P(r,t)$ is the probability described in Section II, which is determined by the distance between the transmitter and receiver, channel environment, the property of receiver, etc. Since the value of N_0 is always large and $|N_0 P(r,t)|$ is not zero, the binomial distribution is approximated as a normal distribution $\mathcal{N}(N_0P(r,t), N_0P(r,t)(1-P(r,t)))$.

Due to the stochastic nature of the molecular movement, a molecule released from a transmitter follows different trajectories before absorbed by a receiver, leading to some molecules emitted earlier arriving later than the ones emitted in the next transmission period, referred to as crossover as well, as depicted in Fig. 2. Therefore, this phenomenon causes severe ISI which increases the error rate and limits the channel capacity. Therefore, the total number of messenger molecules $N_T[n]$ received during the n^{th} symbol interval is mainly composed of three terms: effective signal from the current symbol $N_c[n]$, ISI from the previous symbols $N_p[n]$ and the noise term $N_n[n]$. Then we write $N_T[n]$ as:

$$N_T[n] = N_c[n] + N_p[n] + N_n[n], \tag{19}$$

as mentioned earlier, $N_c[n]$ follows a normal distribution as:

$$N_c[n] \sim \mathcal{N}(N_0 s[n], P_1), \tag{20}$$

where $s[n]$ is the bit sent by the transmitter at the n^{th} symbol interval and $P_1 = P(r, T_s)$. Then we write $N_p[n]$ as:

$$N_p[n] \sim \sum_{i=1}^{I} \mathcal{N}(N_0 s[n-i], q_i), \tag{21}$$

This article has been accepted for publication in a future issue of this journal, but has not been fully edited. Content may change prior to final publication. Citation information: DOI 10.1109/ACCESS.2020.3045439, IEEE Access

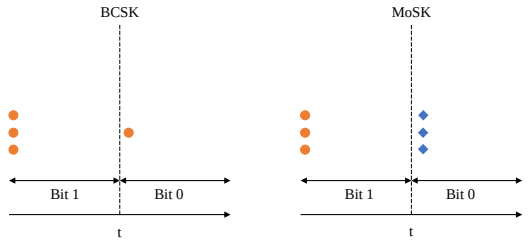

FIGURE 3. A schematic diagram of BCSK and MoSK modulation techniques.

where I is the length of ISI, $s[n-i]$ is the bit sent by the transmitter at the $(n-i)^{th}$ time slot and $q_i = (P_{i+1} - P_i)$. We consider each item in the sum as $N_p[n,i] \sim \mathcal{N}(N_0 s[n-i], q_i)$, then the mean values of $N_p[n,i]$ and $(N_p[n,i])^2$ are derived as:

$$\begin{aligned}\mathbb{E}(N_p[n,i]) &= \pi_0 \mathbb{E}(N_p[n,i]|s[n-i]=0) \\ &\quad + \pi_1 \mathbb{E}(N_p[n,i]|s[n-i]=1) \\ &= N_0 \pi_1 q_i, \end{aligned} \tag{22}$$

$$\begin{aligned}\mathbb{E}((N_p[n,i])^2) &= \pi_0 \mathbb{E}(N_p[n,i])^2|s[n-i]=0) \\ &\quad + \pi_1 \mathbb{E}((N_p[n,i])^2|s[n-i]=1) \\ &= N_0 \pi_1 q_i (1-q_i) + N_0^2 \pi_1 q_i^2, \end{aligned} \tag{23}$$

thus the variance value of $N_p[n,i]$ is derived as follows:

$$\begin{aligned} D(N_p[n,i]) &= \mathbb{E}((N_p[n,i])^2) - \mathbb{E}^2(N_p[n,i]) \\ &= N_0 \pi_1 q_i (1-q_i) + N_0^2 \pi_1 \pi_0 q_i^2 \end{aligned} \tag{24}$$

based on the derivations above, the mean and variance values of $N_p[n]$ are calculated in low computational complexity as:

$$E(N_p[n]) = \sum_{i=1}^{I} N_0 \pi_1 q_i \tag{25a}$$

$$Var(N_p[n]) = \sum_{i=1}^{I} \left(N_0 \pi_1 q_i (1-q_i) + N_0^2 \pi_1 \pi_0 q_i^2 \right), \tag{25b}$$

therefore we write the final form of $N_p[n]$ as:

$$N_p[n] \sim \mathcal{N}(\sum_{i=1}^{I} N_0 \pi_1 q_i, \sum_{i=1}^{I} (N_0 \pi_1 q_i (1-q_i) + N_0^2 \pi_1 \pi_0 q_i^2)) \tag{26}$$

The background noise, also known as signal-independent noise of a MCvD system [28], mainly consists of the random generation and annihilation of messenger molecules, and interference from other communication links utilizing the same type of messenger molecules. The noise originated from these phenomenons is similar to the white noise in wireless communication, which means the noise could be modeled as Additive White Gaussian Noise (AWGN). Hence $N_n[n]$ is a random variable following a normal distribution with zero mean and σ_n standard deviation:

$$N_n[n] \sim \mathcal{N}\left(0, \sigma_n^2\right) \tag{27}$$

B. BCSK

Concentration-based Shift Keying (CSK) is one of the most prevalent modulation techniques used in MCvD systems with the lowest complexity [29], [30], as depicted in the left half of Fig. 3. The transmitter only utilizes one type of messenger molecules, and the receiver decodes the original information by comparing the number of received messenger molecules with proper thresholds. In Binary-CSK (BCSK), only one threshold τ is applied to distinguish two different symbols.

The decision mechanism is as follows:

$$\hat{s}[n] = \begin{cases} 1 & \text{if } N_T[n] \geq \tau \\ 0 & \text{if } N_T[n] < \tau \end{cases} \tag{28}$$

thus we calculate the probabilities of detection and false alarm as:

$$\begin{aligned} &P_{\hat{s},s}(\hat{s}=0|s=0) \\ &= \pi_0 P(N_p + N_n < \tau) \\ &= \pi_0 \left[1 - Q\left(\frac{\tau - \xi}{\sqrt{\eta + \sigma_n^2}} \right) \right], \end{aligned} \tag{29}$$

$$\begin{aligned} &P_{\hat{s},s}(\hat{s}=1|s=0) \\ &= \pi_0 P(N_p + N_n \geq \tau) \\ &= \pi_0 Q\left(\frac{\tau - \xi}{\sqrt{\eta + \sigma_n^2}} \right), \end{aligned} \tag{30}$$

$$\begin{aligned} &P_{\hat{s},s}(\hat{s}=0|s=1) \\ &= \pi_1 P(N_c + N_p + N_n < \tau) \\ &= \pi_1 \left[1 - Q\left(\frac{\tau - N_0 P_1 - \xi}{\sqrt{N_0 P_1 (1-P_1) + \eta + \sigma_n^2}} \right) \right], \end{aligned} \tag{31}$$

$$\begin{aligned} &P_{\hat{s},s}(\hat{s}=1|s=1) \\ &= \pi_1 P(N_c + N_p + N_n \geq \tau) \\ &= \pi_1 Q\left(\frac{\tau - N_0 P_1 - \xi}{\sqrt{N_0 P_1 (1-P_1) + \eta + \sigma_n^2}} \right), \end{aligned} \tag{32}$$

where the values of ξ and η are $\sum_{i=1}^{I} N_0 \pi_1 q_i$ and $\sum_{i=1}^{I} \left(N_0 \pi_1 q_i (1-q_i) + N_0^2 \pi_1 \pi_0 q_i^2 \right)$ as described in (25). $Q(\cdot)$ function is defined as $Q(x) = \frac{1}{2}\text{erfc}(x/\sqrt{2})$.

C. MOSK

Molecular Shift Keying (MoSK) is another frequently-used modulation technique in MCvD systems with a better performance for information transmission and a relatively hight complexity [31], as depicted in the right half of Fig. 3. The transmitter utilizes multiple types of messenger molecules to represent different symbols. It is assumed that all types of molecules have similar properties that they share the same diffusion coefficient and reaction rates.

At the beginning of each time slot, the transmitter releases one of these types of molecules to represent specific information. Then the receiver decodes the original information based on both the concentration and the type of received

TABLE 1. Global Parameters Used in Section IV [10]

Parameter	Value
Viscosity (η)	$0.001kg/sec \cdot m$
Temperature (T)	$310K$
Radius of messenger molecule (r_{mm})	$2.86nm$
Diffusion coefficient (D)	$79.4\mu m^2/s$
Distance between Tx and Rx (d)	$4\mu m$
Radius of Rx (r_{rx})	$10\mu m$
Symbol interval (T_s)	$0.2s$
Number of Molecules for transmitting bit '1' (N_0)	20000
Probability of transmitting bit '1' in BCSK (π_0)	0.5
Probability of transmitting bit '1' in BCSK (π_1)	0.5
Number of types of molecules in MoSK (m)	8
Length of ISI (I)	20

molecules in the current time slot. If the concentration of a certain molecule is higher than the threshold τ while the rest types of the molecules are not, the decoded symbol is related to this particular molecule type.

The correct detection implies that the information detected by the receiver is consistent with the original information in the current time slot. For instance, the transmitter releases type α molecules and the decoding result is α molecule as well. Correspondingly, the false alarm is defined as that the information detected isn't equal to the symbol intended. For example, α molecule is to sent yet β molecule (one of the molecule types utilized except α) is detected.

Thus the probabilities are:

$$
\begin{aligned}
&P_{\hat{s},s}(\hat{s}=\alpha|s=\alpha) \\
&=\frac{1}{m}\left[P(N_c+N_p+N_n\geq\tau)P^{(m-1)}(N_p+N_n<\tau)\right] \\
&=\frac{1}{m}Q\left(\frac{\tau-N_0P_1-\xi}{\sqrt{N_0P_1(1-P_1)+\eta+\sigma_n^2}}\right) \qquad (33) \\
&\cdot\left[1-Q\left(\frac{\tau-\xi}{\eta+\sigma_n^2}\right)\right]^{(m-1)} \qquad (34) \\
&P_{\hat{s},s}(\hat{s}=\beta|s=\alpha) \\
&=\frac{1}{m}\Bigg[P(N_c+N_p+N_n<\tau)P(N_p+N_n\geq\tau) \\
&\cdot P^{(m-2)}(N_p+N_n<\tau)\Bigg] \\
&=\frac{1}{m}\left[1-Q\left(\frac{\tau-N_0P_1-\xi}{\sqrt{N_0P_1(1-P_1)+\eta+\sigma_n^2}}\right)\right] \\
&\cdot Q\left(\frac{\tau-\xi}{\sqrt{\eta+\sigma_n^2}}\right)\left[1-Q\left(\frac{\tau-\xi}{\eta+\sigma_n^2}\right)\right]^{(m-2)} \qquad (35)
\end{aligned}
$$

where m is the number of types of molecules in MoSK, and the values of ξ and η are similar to those in (29)–(32), requiring replacing π_1 and π_0 with $\frac{1}{m}$ and $(1-\frac{1}{m})$.

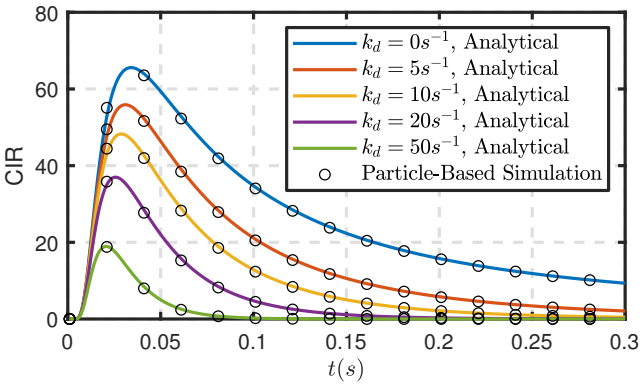

(a) k_d

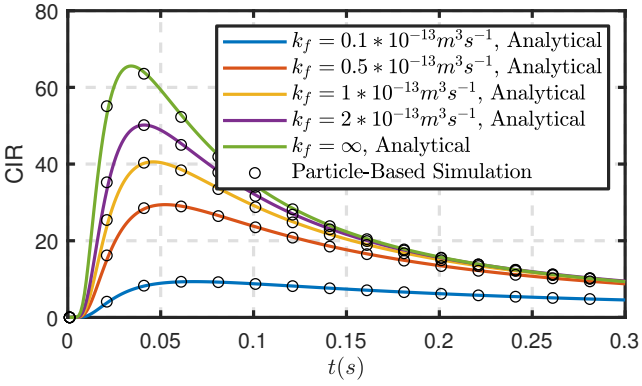

(b) k_f

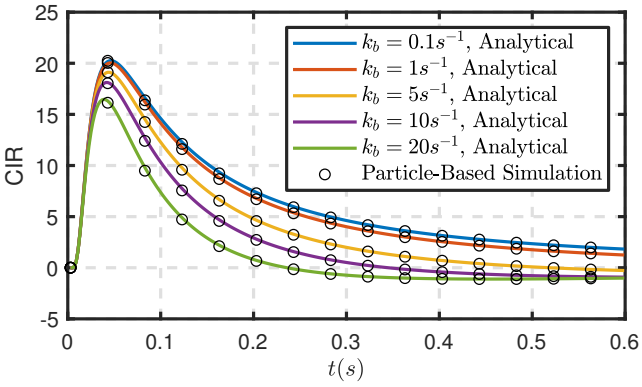

(c) k_b

FIGURE 4. The impact of different reaction rates on CIR.

IV. NUMERICAL RESULTS AND ANALYSIS

Using the conditional probabilities, we define the mutual information $I(X,Y)$ and the channel capacity Cap as [32]:

$$I(X,Y)=\sum_X\sum_Y P(X,Y)\log_2\frac{P(X,Y)}{P(X)P(Y)} \qquad (36)$$

$$Cap=\max_{\tau} I(X,Y) \qquad (37)$$

where $P(X)$ and $P(Y)$ are the probabilities of symbol X transmitted and symbol Y detected. Moreover, we compare the performance of different reaction rates under various

This article has been accepted for publication in a future issue of this journal, but has not been fully edited. Content may change prior to final publication. Citation information: DOI 10.1109/ACCESS.2020.3045439, IEEE Access

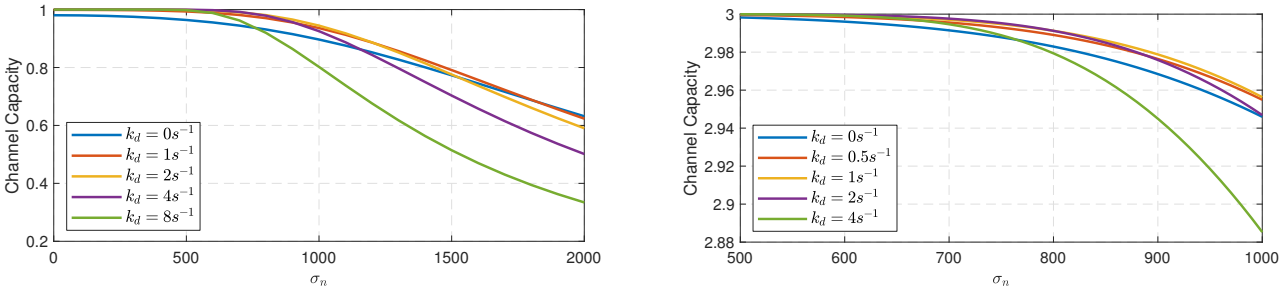

(a) BCSK (b) MoSK

FIGURE 5. The impact of degradation reaction rate k_d on channel capacity for BCSK and MoSK.

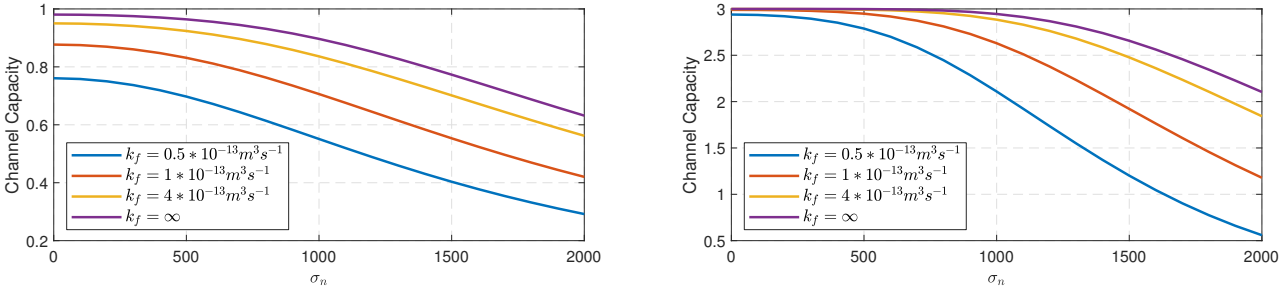

(a) BCSK (b) MoSK

FIGURE 6. The impact of forward reaction rate k_f on channel capacity for BCSK and MoSK.

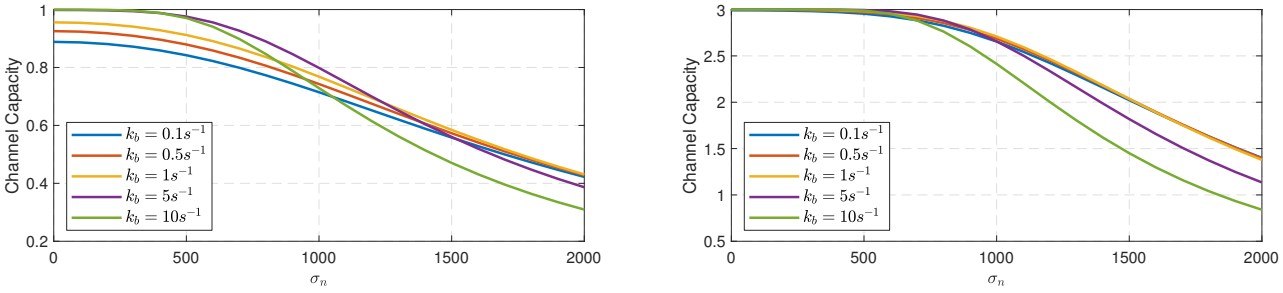

(a) BCSK (b) MoSK

FIGURE 7. The impact of backward reaction rate k_b on channel capacity for BCSK and MoSK.

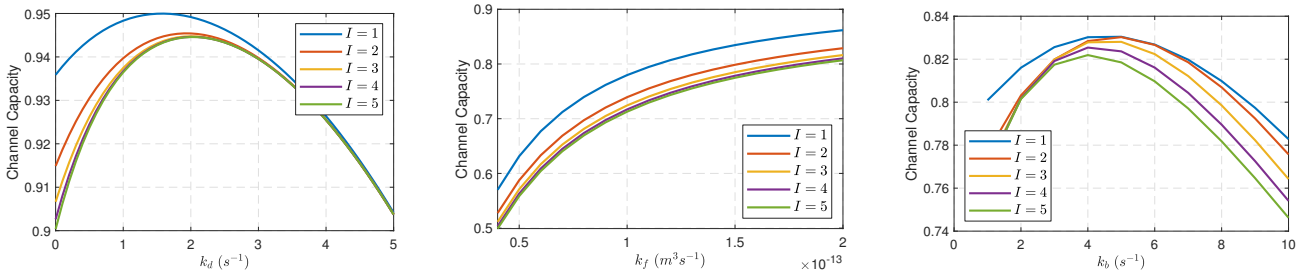

(a) k_d (b) k_f (c) k_b

FIGURE 8. The impact of different reaction rates on channel capacity for BCSK with various length of ISI.

noise levels. The channel capacity performance of BCSK and MoSK at different reaction rates is evaluated in the comprehensive MCvD system model with a first-order degradation reaction and a second-order reversible reaction as elaborated

This article has been accepted for publication in a future issue of this journal, but has not been fully edited. Content may change prior to final publication. Citation information: DOI 10.1109/ACCESS.2020.3045439, IEEE Access

in Section II. Unless explicitly noted, numerical results are obtained from the parameters listed in Table 1 and all the results are validated by averaged particle-based simulations [33].

In Fig. 4(a), we apply the settings as in the first case in Section II-B with $k_f \to \infty$ and $k_b = 0$. It is shown that the simulation results are in good agreement with the results obtained by analytical calculations. Besides, it is observed that with the increase of degradation reaction rate k_d, the CIR decreases. This is mainly because that the degradation of messenger molecules results in a reduction of the number of messenger molecules in the channel, and then causes a reduction of the number of molecule C at the receiver. At the same time, the ISI of molecular signal also decreased with the increase of k_d, and the ISI could be even completely eliminated when k_d is large enough ($k_d > 10s^{-1}$).

In Fig. 4(b), we apply the settings as in the second case in Section II-B with $k_d = 0$ and $k_b = 0$. As can be seen from Fig. 5, the CIR increases with the increase of forward reaction rate k_b. In addition, when k_f is relatively large ($k_f > 0.5 \times 10^{-13} m^3 s^{-1}$), the increase of k_f does not result in a significant increase in ISI.

In Fig. 4(c), we apply the settings as in the third case in Section II-B with $k_d = 0$ and $k_f = 1 \times 10^{-13} m^3 s^{-1}$. It is shown that the increase of backward reaction rate k_b leads to a reduction of CIR, and even negative values of CIR appear when k_b and t are large enough. The negative CIR indicates that the number of messenger molecules dissociated from receptors is larger than the number of messenger molecules combined with receptors at certain time.

Fig. 5 depicts the channel capacity for BCSK and MoSK under different k_d. It is shown that the channel capacity decreases with the increase of background noise σ_n. The maximum channel capacity that could be achieved for BCSK is 1 and for MoSK is $\log_2 m = 3$, which is consistent with the law of Shannon channel. The channel capacity increases with a larger value of k_d when σ_n is relatively small, which is benefit from the degradation reaction that reduces the ISI. However, the result is quite the reverse when σ_n is relatively large. This is because the effective signal that could be received is reduced under this circumstance, resulting in the reduction of Signal-to-Noise Ratio (SNR), thus reducing the channel capacity.

Fig. 6 depicts the channel capacity for BCSK and MoSK under different k_f. It is shown that the channel capacity increases monotonically with the increase of k_f, and this trend is independent with σ_n. This phenomenon is consistent with Fig. 4(b) that the increase of k_f leads to a larger effective signal and thus improves the SNR without great impact on ISI.

Fig. 7 depicts the channel capacity for BCSK and MoSK under different k_b. It can be seen from Fig. 7 that the phenomenon is similar to that in Fig. 5 that the channel capacity does not increase monotonically with the increase of k_b and the influence of background noise should be considered.

In addition, a comprehensive observation of Fig. 5, Fig. 6 and Fig. 7 shows that under the same noise and reaction rate conditions, the channel capacity of MoSK is closer to the theoretical maximum capacity than that of BCSK, which indicates that MoSK is more resistant to noise and ISI.

The length of ISI considered in the above simulation results and analysis is long ($I = 20$), while in practical channel estimation and signal detection, the length of ISI is usually set to a smaller value. This is because the value of ISI gradually decreases over time, therefore only the first few bit intervals of ISI ($I \leq 3$) affects the molecular signal significantly. Without losing generality, Fig. 8 depicts the channel capacity under various reaction rates with different length of ISI for BCSK. As can be seen from Fig. 8(a) and (b), with the increase of I, the channel capacity gradually approaches to a constant. Besides, when k_d is large enough, only the first bit interval of ISI has an affect on the channel capacity. However, no similar phenomenon is observed with the increase of k_f, which further indicates that the inhibition ability of degradation reaction on ISI is stronger.

It is shown from Fig. 8(c) that when k_b is relatively small ($0 < k_b < 2.5s^{-1}$), the channel capacity is influenced by a smaller length of ISI. However, when k_b is larger enough ($k_b \geq 8s^{-1}$), each bit interval of ISI has an obvious impact on channel capacity. This is mainly because the appearance of negative ISI. It can be seen from Fig. 4(c) that this negative ISI will exist for a long period of time. Therefore, in this case, the length of ISI to be considered should be appropriately increased when channel estimation and channel capacity calculation are implemented.

V. CONCLUSION

In this paper, a comprehensive molecular channel model with a first-order degradation reaction in the channel and a second-order reversible reaction at the receiver side is investigated. The CIR of this channel model is provided and decoupled into three cases to investigate the impacts of different reaction rates respectively. Subsequently, each component of molecule signal is quantified by Gaussian approximation, including effective signal from the current symbol, ISI from previous symbols and background noise. On this foundation, we derive the correct and false detection probability under BCSK and MoSK modulation techniques to obtain the channel capacity. From the numerical results, it is observed that the CIR and channel capacity could be significantly influenced by reactions. The selection of messenger molecules according to the environment and the receiver with proper reaction rates (e.g., a relatively large forward reaction rate k_f) is critical to the performance of information transmission for MCvD. Besides, the effective length of ISI is also subject to the reaction rates such as the increase of degradation rate k_d and forward reaction rate k_f could mitigate ISI markedly. In our future work, the realization of physical protype for the biological channel by utilizing nano-machines is our next research direction.

REFERENCES

[1] N. Farsad, H. B. Yilmaz, A. Eckford, C. B. Chae, and W. Guo, "A comprehensive survey of recent advancements in molecular communication," IEEE Communications Surveys Tutorials, vol. 18, no. 3, pp. 1887–1919, thirdquarter 2016.

[2] M. Kuscu, E. Dinc, B. A. Bilgin, H. Ramezani, and O. B. Akan, "Transmitter and receiver architectures for molecular communications: A survey on physical design with modulation, coding and detection techniques," Proceedings of the IEEE, vol. PP, no. 99, pp. 1–40, 2019.

[3] Pierobon and Massimiliano, "Fundamentals of diffusion-based molecular communication in nanonetworks," Foundations & Trends in Networking, vol. 8, no. 1-2, pp. 1–147, 2012.

[4] T. Nakano, A. W. Eckford, and T. Haraguchi, Molecular Communication. Cambridge University Press, 2013.

[5] Z. Wei, B. Li, C. Sun, and W. Guo, "Sampling and inference of networked dynamics using log-koopman nonlinear graph fourier transform," IEEE Transactions on Signal Processing, vol. 68, pp. 6187–6197, 2020.

[6] Z. Wei, B. Li, W. Guo, W. Hu, and C. Zhao, "Sequential bayesian detection of spike activities from fluorescence observations," IEEE Transactions on Molecular, Biological and Multi-Scale Communications, vol. 5, no. 1, pp. 3–18, 2019.

[7] W. Guo, C. Mias, N. Farsad, and J. Wu, "Molecular versus electromagnetic wave propagation loss in macro-scale environments," IEEE Transactions on Molecular, Biological and Multi-Scale Communications, vol. 1, no. 1, pp. 18–25, 2015.

[8] B. Alberts, "Essential cell biology," Molecular Reproduction & Development, vol. 51, no. 4, pp. 477–477, 2015.

[9] M. U. Mahfuz, D. Makrakis, and H. T. Mouftah, "A comprehensive study of sampling-based optimum signal detection in concentration-encoded molecular communication," IEEE Transactions on NanoBioscience, vol. 13, no. 3, pp. 208–222, Sept 2014.

[10] H. B. Yilmaz, A. C. Heren, T. Tugcu, and C. B. Chae, "Three-dimensional channel characteristics for molecular communications with an absorbing receiver," IEEE Communications Letters, vol. 18, no. 6, pp. 929–932, June 2014.

[11] M. Pierobon and I. F. Akyildiz, "Noise analysis in ligand-binding reception for molecular communication in nanonetworks," IEEE Transactions on Signal Processing, vol. 59, no. 9, pp. 4168–4182, Sept 2011.

[12] H. ShahMohammadian, G. G. Messier, and S. Magierowski, "Modelling the reception process in diffusion-based molecular communication channels," in 2013 IEEE International Conference on Communications Workshops (ICC), June 2013, pp. 782–786.

[13] Y. Deng, A. Noel, M. Elkashlan, A. Nallanathan, and K. C. Cheung, "Modeling and simulation of molecular communication systems with a reversible adsorption receiver," IEEE Transactions on Molecular, Biological and Multi-Scale Communications, vol. 1, no. 4, pp. 347–362, Dec 2015.

[14] A. Akkaya, H. B. Yilmaz, C. B. Chae, and T. Tugcu, "Effect of receptor density and size on signal reception in molecular communication via diffusion with an absorbing receiver," IEEE Communications Letters, vol. 19, no. 2, pp. 155–158, Feb 2015.

[15] A. Noel, K. C. Cheung, and R. Schober, "Improving receiver performance of diffusive molecular communication with enzymes," IEEE Transactions on NanoBioscience, vol. 13, no. 1, pp. 31–43, March 2014.

[16] A. C. Heren, H. B. Yilmaz, C. B. Chae, and T. Tugcu, "Effect of degradation in molecular communication: Impairment or enhancement?" IEEE Transactions on Molecular, Biological and Multi-Scale Communications, vol. 1, no. 2, pp. 217–229, June 2015.

[17] Y. J. Cho, H. B. Yilmaz, W. Guo, and C. Chae, "Effective inter-symbol interference mitigation with a limited amount of enzymes in molecular communications," Transactions on Emerging Telecommunications Technologies, 2016.

[18] Y. J. Cho, H. B. Yilmaz, W. Guo, and C. B. Chae, "Effective enzyme deployment for degradation of interference molecules in molecular communication," in 2017 IEEE Wireless Communications and Networking Conference (WCNC), March 2017, pp. 1–6.

[19] A. Ahmadzadeh, H. Arjmandi, A. Burkovski, and R. Schober, "Comprehensive reactive receiver modeling for diffusive molecular communication systems: Reversible binding, molecule degradation, and finite number of receptors," IEEE Transactions on NanoBioscience, vol. 15, no. 7, pp. 713–727, Oct 2016.

[20] D. Kilinc and O. B. Akan, "Receiver design for molecular communication," IEEE Journal on Selected Areas in Communications, vol. 31, no. 12 Partsupplement, pp. 705–714, 2013.

[21] A. Noel, K. C. Cheung, and R. Schober, "Optimal receiver design for diffusive molecular communication with flow and additive noise," IEEE Transactions on NanoBioscience, vol. 13, no. 3, pp. 350–362, 2014.

[22] H. C. Berg, "Random walks in biology," Physics Today, vol. 40, no. 3, pp. 73–74, 1987.

[23] V. Jamali, A. Ahmadzadeh, W. Wicke, A. Noel, and R. Schober, "Channel modeling for diffusive molecular communication–a tutorial review," Proceedings of the IEEE, vol. 107, no. 99, pp. 1256–1301, 2019.

[24] W. Guo, Y. J. Cho, C. B. Chae, and H. B. Yilmaz, "Interference reduction via enzyme deployment for molecular communication," Electronics Letters, vol. 52, no. 13, 2016.

[25] J. Sun and H. Li, "Expected received signal in diffusive molecular communication with finite binding receptors," IEEE Communications Letters, vol. 24, no. 12, pp. 2829–2833, 2020.

[26] S. S. Andrews, "Accurate particle-based simulation of adsorption, desorption and partial transmission," Physical Biology, vol. 6, no. 4, p. 046015, 2009.

[27] Cubic Equation. John Wiley & Sons, Inc., 2005.

[28] S. Liu, Z. Wei, B. Li, W. Guo, and C. Zhao, "Metric combinations in non-coherent signal detection for molecular communication," Nano Communication Networks, vol. 20, 2019.

[29] Z. Wei, W. Guo, B. Li, J. Charmet, and C. Zhao, "High-dimensional metric combining for non-coherent molecular signal detection," IEEE Transactions on Communications, vol. 68, no. 3, pp. 1479–1493, 2020.

[30] S. Liu, Z. Wei, B. Li, and C. Zhao, "Unsupervised clustering-based non-coherent detection for molecular communications," IEEE Communications Letters, vol. 24, no. 8, pp. 1687–1690, 2020.

[31] M. S. Thakur and V. Bhatia, "Performance analysis of flow assisted diffusion based molecular communication for d-mosk," in 2018 IEEE 87th Vehicular Technology Conference (VTC Spring), 2018, pp. 1–6.

[32] G. Alfano and D. Miorandi, "On information transmission among nanomachines," in 2006 1st International Conference on Nano-Networks and Workshops, Sept 2006, pp. 1–5.

[33] S. S. Andrews and D. Bray, "Stochastic simulation of chemical reactions with spatial resolution and single molecule detail," Physical Biology, vol. 1, no. 3, pp. 137–151, aug 2004.